Unsharp Masking with Histogram Equalization for Remote Sensing Image Enhancement

Shubhi Kansal
Assistant Professor, Department of Electronics and Communication Engineering, Madhav Institute of Technology and Science, Gwalior, India

Abstract
A crucial aspect of image enhancement is contrast enhancement. As remote sensing photos are taken from a distance, they naturally have much lower contrast than other types of images. Although techniques for improving remote sensing images have been developed in recent years, it is still unknown how well and consistently these techniques work for contrast enhancement. In this letter, a novel unsharp mask filtering method that combines histogram equalization with the image's maximum detail is suggested. This method visually enhances the image considerably more effectively than any other method now in use. The image is first sharpened by using an unsharp mask filter. After that, a cutting procedure is used to prevent the over-enhancing of the image. Then, using the mean as a guide, the histogram equalization procedure is carried out, and finally, the unsharp mask filter is once more utilized to produce the visually sharpened and enhanced image.

Keywords: Unsharp masking, Sharpening, Clipping

1. Introduction

In order to produce a better output image, the image enhancement method modifies the pixel intensity [1-2]. Because of its numerous applications in the fields of military operations, historical surveying, disaster monitoring, coastal land use and regulation, etc., remote sensing images require significant improvement [3–7]. Due to their far capture and environmental settings, remote sensing photos have a reduced contrast. Histogram equalization (HE), a straightforward and effective method for improving images, is frequently utilized. While using HE, the transformation function is used to boost the image's contrast.

When HE is used, there are some disadvantages, though. The image's average brightness is off, and the upgraded version of the image might have some artefacts.

Another technique for enhancing remote sensing images was put forth in 2010 and is known as SEDWT-SVD (Satellite Image Contrast Enhancement Using Discrete Wavelet Transform and Regular Value Decomposition) [8]. This technique is a method of domain transformation that divides the input photograph into DWT subbands while maintaining the brightness of the image via single value decomposition. This strategy had the problem of making the image's total information content less.

It was suggested in 2011 [9] to improve optical remote sensing images using subband decomposed multiscale retinex with hybrid intensity transfer function. Based on multiscale retinex, this approach (MSR). The image was split up into multiple sub bands, making it a rather difficult process even though it gave good results.

It was suggested to use Exposure-based sub-image histogram equalization (ESIHE) in 2014 [10]. This method involves calculating a clipping threshold and histogram clipping in accordance with the estimated clipping threshold. The image's mean brightness is not preserved by ESIHE; it merely controls enhancement. Also, it added noise to some of the photographs.

Global and local contrast enhancement processes were used in the regularized- histogram equalization and discrete cosine transform (RHEDCT) methods that were proposed in 2015 [11]. The entropy and contrast enhancement results of this method were good but it introduced noise in the enhanced images.

An effective contrast enhancement method for remote sensing images (HCTLS)[12] was proposed in 2017. For the purpose of improving remote sensing photos, this method utilised linear stretching and histogram compacting transform. Although the approach was robust, it fell short of revealing all of the image's information. In comparison to RHEDCT and the suggested approach, the enhanced image's entropy and enhancement measurement (EME) values were similarly lower.

A global local image enhancement (GLIE)[13] was proposed in 2021. This method employed weighted least square method for the purpose of contrast improvement. This method very well enhanced the details but failed to preserve the brightness of the images.

An adaptive enhancement algorithm (AEA)[14] based on feature fusion was proposed in 2022 for high resolution satellite images. The method provided better enhancement effect as well as shorter enhancement time but could not improve the sharpness of the images.

The strategy suggested in this study produces a high-quality visual image and extracts the most information possible from the image while overcoming the shortcomings of the techniques listed above. An unsharp mask filter is used to enhance the image's sharpness. The image histogram is clipped after the sharpening operation. Clipping techniques prevent the image from being over- or under-edited. Following the application of histogram equalization based on the mean, the image that has been histogram equalized is once more sharpened using a filter to produce the enhanced image. The issue of image brightness excessive augmentation, or halo artefacts are not

present in this improved image. To validate the effectiveness of the suggested method and demonstrate that our method outperformed all existing methods, various parameters including entropy, enhancement factor, mean gradient, and Naturalness Image Quality Evaluator (NIQE) have been tested and compared with RHEDCT (2015), HCTLS (2017), GLIE (2021) and AEA (2022) existing methods. The proposed method's visual and objective outcomes can also improve the categorization accuracy of the photos.

2. Motivation

The reason behind proposing this particular strategy is to prevent the under and over enhancement issue that is present in most of the HE methods previously presented. Unlike other HE systems, this one can effectively maintain the image brightness while also preventing artefacts in the enhanced image. The approach is also recommended since it has a good chance of bringing out the image's details, which can improve image categorization.

Another crucial point is that unsharp masking was used to sharpen the images rather than a traditional high pass filter like the Laplacian. There are two causes for this.

-Halo artefacts are created in the image when sharpening is done directly using high pass filter.

-According to the type of image being enhanced, unsharp masking's variable parameters can be changed.

Let, Iin(m, n) is the given input image. Firstly, we calculate a blurred or smoother image Ismooth(m, n) through a Gaussian linear filter which is applied on Iin(m, n). After that the sharped image which we obtain is

$$Isharp = Iin(m, n) + c.(Iin(m, n) - Ismooth(m, n)) \quad (1)$$

where $0 \leq c \leq 1$. Hence, the value of c is variable. On the other hand the equation used for sharpening of image by laplacian filter is given as

$$Isharp = Iin\ (m, n) - \Delta Iin(m, n). \quad (2)$$

It is clear that equation (2) contains no variables or parameters. This was the driving force for employing the unsharp masking technique rather than a high pass filter since it can be used to a variety of remote sensing image types.

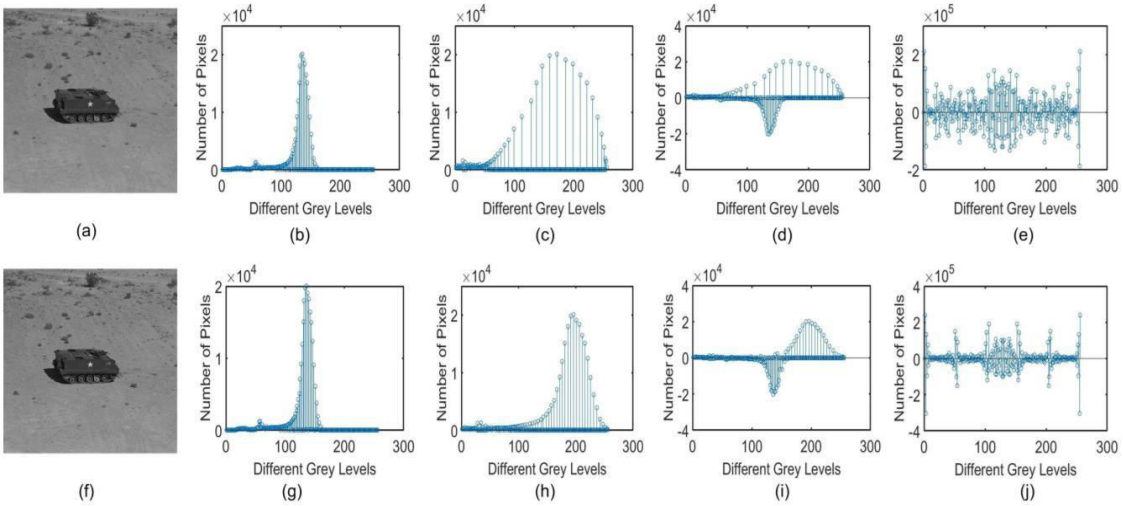

Figure 1: Tank image: (a) Original image (b) Image histogram (c) HE enhanced image histogram (d) Difference between (c) and (b) (e) FFT of (d) (f) Input sharpened image (g)Histogram of sharpened image (h) Histogram of enhanced sharped image combined with HE (i) Difference between (h) and (b) (j) FFT of (i)

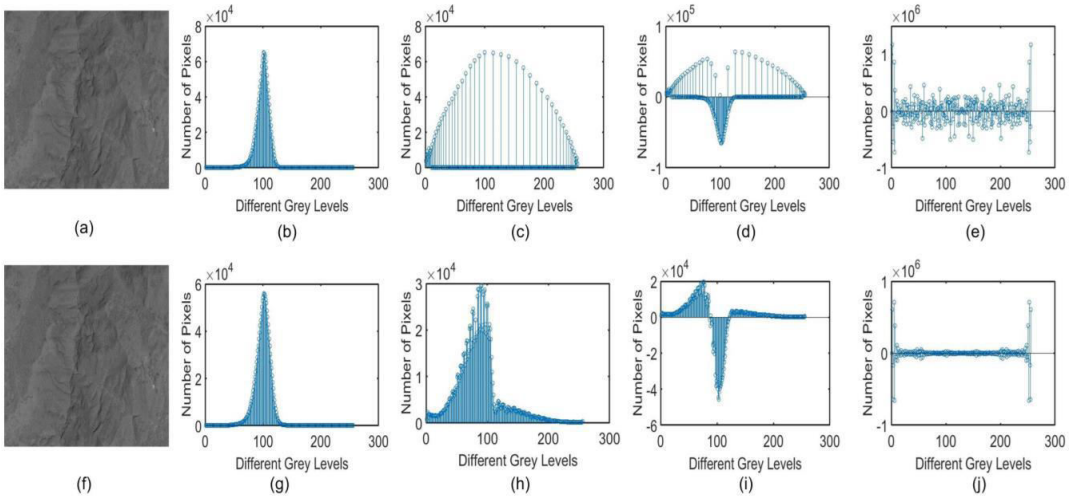

Figure 2: GF-1 image: (a) Original image (b) Image histogram (c) HE enhanced image histogram (d) Difference between (c) and (b) (e) FFT of (d) (f) Input sharpened image (g)Histogram of sharpened image (h) Histogram of enhanced sharped image combined with HE (i) Difference between (h) and (b) (j) FFT of (i)

Fig.1 and Fig.2 shows the histogram results of Tank and GF-1 Image at various phases. These two figures explain the concept of combining the Sharpening procedure with HE. The input Tank image is shown in Fig.1(a). The histogram of the input image is shown in Fig.1(b). Fig.1(c) is the result of applying HE on the input image. The histogram in Fig.1(d) is the difference between Fig.1(c) and Fig.1(b). The FFT computed for the Fig.1(d) is shown in Fig.1(e).

The sharpened input image is shown in Fig.1(f). The histogram of Fig.1(f) is shown in Fig.1(g). It is evident that the sharpening procedure just sharpens the image, but when combined with HE, it can also expand the dynamic range of the image, offering overall enhancement, as seen in Fig.1(h). The difference between Fig.1(h) and Fig.1(b) is shown by the histogram in Fig.1(i). When we compare Fig.1(i) and Fig.1(d), we can see that the change in the number of pixels in the y-direction is smoother in Fig.1(i) than in Fig.1(d). Further oscillations in the number of pixels are produced in Fig.1(d). In Fig.1(i) between 100 to 150, first of all the pixel change is in negative direction continuously and than from

150 onwards in positive direction continuously. In Fig.1(d) between 50 to 150,there are random changes in pixels, i.e. some portions are positive while some are negative which is not desired. This is also evident in Fig.1(e) and Fig.1(j), which are FFTs of Fig.1(d) and Fig.1(i), respectively. The oscillation in Fig.1(e) is excessively high in comparison to Fig.1 (j). As a result, the improved image created by the HE approach has artefacts. The results for Fig.2 are similar. As a result, this was the impetus for developing this technique.

3. Proposed Methodology

The flowchart depicts the steps of the proposed algorithm in Fig.3:

3.1. Sharpening of the Image

Essentially, sharpening is a technique to increase an image's apparent sharpness. It describes the image's finer elements, particularly those that the observer would overlook [15].

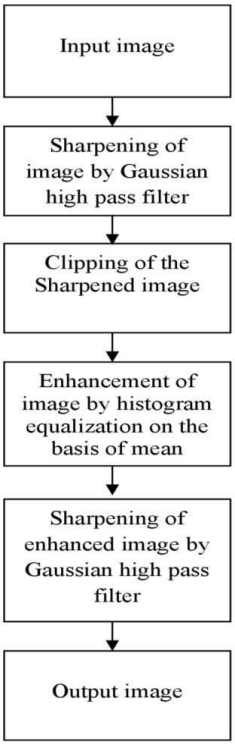

Figure 3: Flowchart of the proposed method

Sharpening is done in this case using the Unsharp masking approach. To discover all the edges, the original image is essentially subtracted from a blurred (unsharp) duplicate. This edge information is used to build a mask. The total impact is then made relevant to the original image after the edges contrast is increased.
To create an unsharp mask, the specimen picture is filtered spatially with a Gaussian filter[16][17]. This filter can be thought of as a two-dimensional Gaussian function produced by the convolution of an image with a kernel mask.

The σ parameter sets the size of the Gaussian kernel mask, which determines the frequency range rejected by the Gaussian filter.

3.2. Clipping Threshold

Image histogram is now constructed and cropped to neglect the enhancement effects caused by the standard HE approaches after the image has been

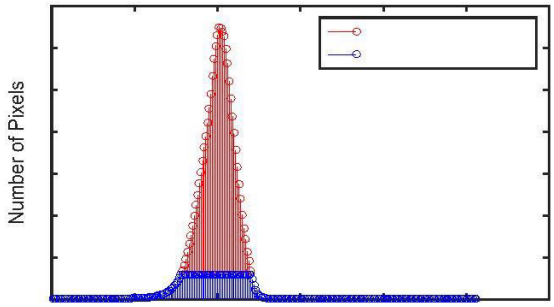

Different Grey Levels

Figure 4: Clipped Histogram image of GF-1

sharpened using the aforementioned procedure. The mean of the grey level occurrences is used to calculate the clipping threshold in this case. Because of its effectiveness and quick speed, this particular method of histogram cutting was chosen. Let F be the filtered picture, and the range of the gray values be

$$0 \text{ to } L\text{-}1(F_0, F_1, \ldots, F_i, F_{L-1}).$$

The histogram of the filtered image is H(F)= (no, n1, ..., ni, ..., nL–1) where ni is the number of pixels with i gray level. Let N is total number of pixels in image Clipped Histogram is calculated as:

$$HC(F) = CT \text{ , if}(H(F) > CT) \quad (3)$$

where CT is clipping threshold. Fig.4 shows the original and clipped histogram for the GF-1 image used in this paper. The clipping operation smooths the part of the histogram with peaks, while the rest is overlapped, as seen in the image.

3.3. Segmentation Cutoff

The histogram (HC(F)) which was clipped is divided into halves based on the mean intensity value, as in the Bi-histogram Equalization (BBHE) [18] approach. Let Fm be the clipped histogram's mean intensity value. As a result, histogram subdivision is performed with Fm, and this procedure yields two sub pictures, Fl and Fu.

$$HC(F) = Fl \cup Fu \quad (4)$$

where

$$Fl = (F(m, n) \leq Fm) \quad (5)$$

$$Fu = (F(m, n) > Fm) \quad (6)$$

The sub image Fl composed of (Fo, F1, …, Fm) and the other sub image Fu composed of (Fm+1, Fm+2, …FL–1).

3.4. Equalization Process

The two sub-images are subjected to the histogram equalization method following the segmentation of the clipped histogram. Transform functions in terms of Cumulative density functions (CDF):

$$TL(Fi) = Fo + (Fm - Fo) * CL(Fi) \quad (7)$$

$$TU(Fi) = Fm+1 + (FL-1 - Fm+1) * CU(Fi) \quad (8)$$

where CL(Fi) and CU (Fi) are CDF of Fl and FU sub image respectively. Transform function of the image is given by TF

$$TF = TL(Fi) \cup TU(Fi) \quad (9)$$

A final enhanced image is created by applying a gaussian filter once more to the TF image that was acquired in section 1 above in order to sharpen it.

4. Evaluating Parameters

Without quantitative evaluation, picture improvement is not possible, and method validity cannot be demonstrated. In this research four parameters are used for the assessment. The first one is discrete entropy (E) [19]. It is simply the quantity of information (in the Shannon sense) required to specify the images details. The higher value of entropy indicates a image with high contrast.

Other one is the enhancement factor (EME) [20]. The amount by which the processed image has been improved over the original image is indicated. The third parameter that is measured here is mean gradient (MG) [12]. It gives the value of local contrast enhancement of the image. Basically, if the value of mean gradient is high for an image than it indicates superior quality of the image.

The Naturalness Image Quality Evaluator (NIQE) is the fourth criteria that is assessed here [21]. It is a statistic for no-reference quality evaluation. In order to function, NIQE relies on statistical regularities that are derived from real, distortion-free images. Basically, “quality aware” attributes are gathered and used to a multivariate Gaussian (MVG) model to create the NIQE.

Regular natural scene statistics model (NSS) are used to obtain the quality aware properties. The difference between an MVG fit of the NSS attributes derived from the test picture and an MVG model of the quality aware attributes collected from the natural images is then used to calculate the quality score of any image. NIQE value for an image should be as low as possible.

5. Results and Analysis

In this paragraph we provide both quantitative as well as quality assessment of images taken in this paper and compared with the other methods as discussed in the introduction section. Four images from [6], two images from [13] and 24 images were collected from the standard Computer vision group (CVG-UGR) database, totaling 30 satellite images. A total of 30 images were captured for testing.

5.1. Quantitative Evaluation

Table.1 displays the findings for various images and methodologies. Proposed method provides entropy values for Mars, GF-1, Sat and Tank image 4.40, 7.08, 7.27 and 7.31 respectively which is highest among all. Comparing to it GLIE has second highest values for entropy. This outcomes shows that information present in our enhanced images is best. Next, the EME values for Mars,GF-1, Sat and Tank image are 25.75, 20.73, 34.90, 17.16 respectively which is also highest. This parameter confirms that the degree of enhancement is best in our technique. HCTLS method has the second highest values for EME. Mean gradient (MG) values for Mars image is 11.56, GF-1 is 13.21, Sat is 15.93 and
tank image is 17.21 respectively. These values indicates that our enhanced image is of better quality than all the other enhanced images. Lastly, as explained in section 4 that NIQE value should be minimum, proposed method is giving the minimum values. For Mars NIQE is 3.92, for GF-1 is 4.45, for Sat is 4.50 and for tank image is 3.89. From these results we can also conclude that the

Table 1: Various Parameter measures

Image	Methods	Entropy	EME	MG	NIQE
Mars	Original Image	3.08	-	8.31	5.00
	RHEDCT	3.02	10.99	9.54	5.27
	HCTLS	3.07	21.72	10.62	4.76
	GLIE	4.35	14.32	7.44	4.79
	AEA	3.07	17.74	10.17	4.80
	Proposed	4.40	25.75	11.56	3.92
GF-1	Original Image	5.39	-	3.62	4.69
	RHEDCT	5.27	15.56	8.72	4.51
	HCTLS	5.36	19.83	10.52	4.57
	GLIE	7.03	18.59	12.32	4.71
	AEA	5.37	18.24	11.34	4.49
	Proposed	7.08	20.73	13.21	4.45
Satellite	Original Image	6.96	-	12.70	5.28

	RHEDCT	6.70	25.55	10.35	5.32
	HCTLS	6.95	34.04	12.38	5.31
	GLIE	7.20	30.41	13.41	5.30
	AEA	6.96	27.65	14.35	5.11
	Proposed	7.27	34.90	15.93	4.50
Tank	Original Image	5.05	-	5.27	4.09
	RHEDCT	5.01	6.45	6.87	4.02
	HCTLS	5.06	15.59	7.53	3.95
	GLIE	6.58	7.91	9.83	4.03
	AEA	5.07	6.56	7.68	4.05
	Proposed	7.31	17.16	17.21	3.89

Table 2: Average computation time (in sec)

Image Size	RHEDCT	HCTLS	GLIE	AEA	Proposed
256 x 256	0.15	15.67	0.95	9.82	0.12
387 x 382	0.22	17.53	1.78	11.89	0.19
512 x 512	0.35	19.78	2.22	13.21	0.32
548 x 548	0.51	22.39	2.54	14.87	0.49
1500 x 1000	1.38	40.35	5.59	18.54	1.12

proposed method maintains robustness for various types of images. The results for the computational complexity of various approaches are displayed in Table.2. The average computation time is shown in seconds. Results are displayed for photos of various sizes. As can be seen, the proposed method processes the image in the shortest amount of time. RHEDCT is also quite similar to the suggested approach.

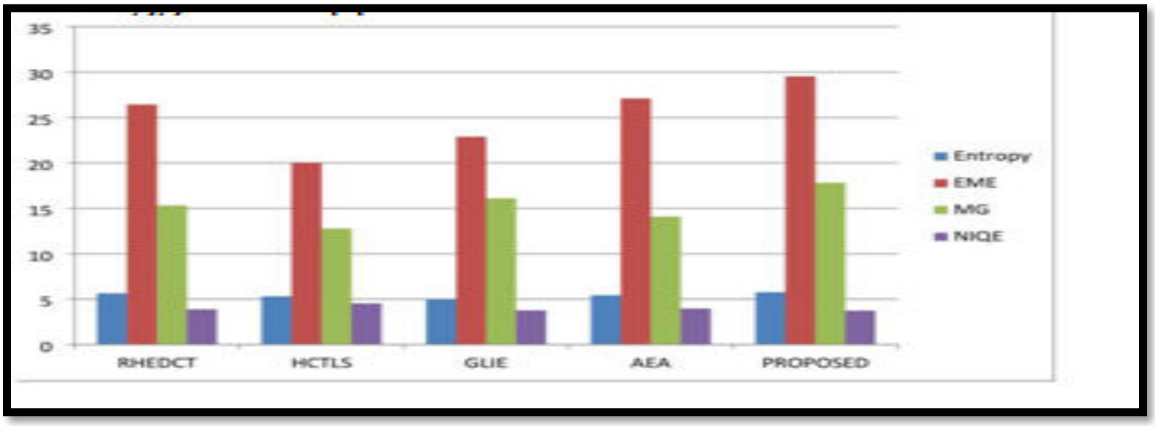

Figure 5: Average Result of 30 images for different methods

Fig.5 shows the average result for all the 30 images in a form of bar chart. Blue bar shows the result for entropy. As it can be seen that proposed method gives the highest average entropy. RHEDCT method gives the second highest value of entropy. Red bar gives the result for EME. Again, proposed method shows the highest enhancement and AEA method second highest. Green bar shows the result for MG and violet bar shows the result for NIQE. MG and NIQE results are also the best for proposed method as compared to all the other methods.

5.2. Visual Quality Assessment

To analyze an image visual judgment of the image is very important. In this paper visual analysis of four images are described from different database so as to proof that our method is working well for different images. Fig.7 is panchromatic images taken from the [12]. Fig.6, Fig.8 and Fig.9 are obtained from the standard Computer vision group (CVG-UGR) database image database. Fig.6 (b)-(f) shows the image enhancement results for Mars image. If the overall image is analyzed than it can be seen that the image was brightened out too much and only very little portion in the right hand side corner gives details.

Hence RHEDCT results made the upper part of the image more dark and the information in the image was not clear. HCTLS enhanced the image but it added some additional noise.

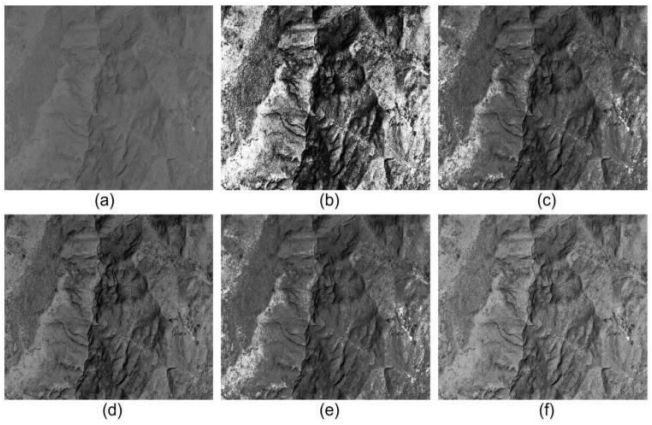

Figure 6: Mars: (a) Original (b) RHEDCT (c) HCTLS (d) GLIE (e) AEA (f) Proposed

The visual results of GLIE was not very pleasing. AEA and proposed method both produced better image in terms of brightness as well as contrast. Proposed method provides the better details in the image.

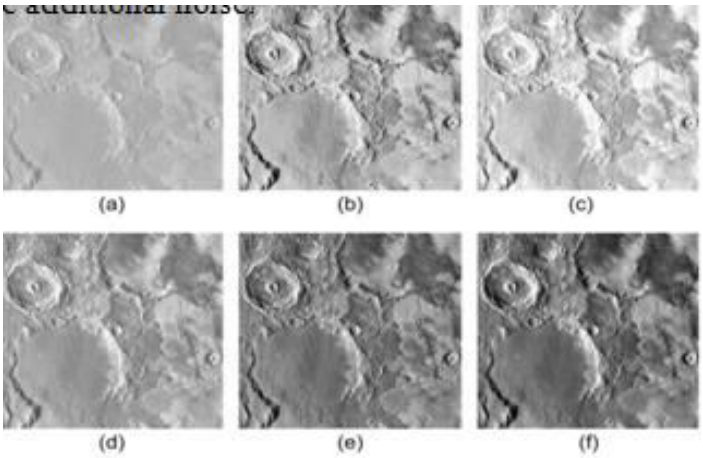

Figure 7: GF-1: (a) Original (b) RHEDCT (c) HCTLS (d) GLIE (e) AEA (f) Proposed

Fig. 7(b)-(f) shows the results for GF-1 image. The appearance of the original image is very less bright. RHEDCT enhanced the image but it added noise and artifacts to most parts of the image. HCTLS and GLIE enhanced the image upto good extent but they also introduced noise in some areas of the image as it can be seen clearly. The AEA results for this image was comparatively very good. The image was enhanced both globally and locally very well. Proposed method gave more pleasing results if compared to AEA as well. Each and every detail of the image was very clearly visible. Fig.8 (b)-(f) shows the results for Satellite image. As compared to the original image RHEDCT method produced too much noise in the complete image. HCTLS has disturbed the brightness of the image. The image enhanced by GLIE is somewhat blurred and does not provide the clear details. AEA method failed to enhance this particular image. In the proposed method surface can be seen clearly both in dark and bright parts. This method has properly adjusted the intensity level of the original image. Fig.9(b)-(f) shows the results for tank image. The tank image enhanced by the RHEDCT method again introduced too much of artifacts. HCTLS and GLIE enhanced the image upto some level but the results were not very attractive. AEA produced good enhancement result for this image but if observed carefully the image became over bright due to which some minute details were lost. Proposed method enhancement made clearly visible the tank as well as its surroundings.

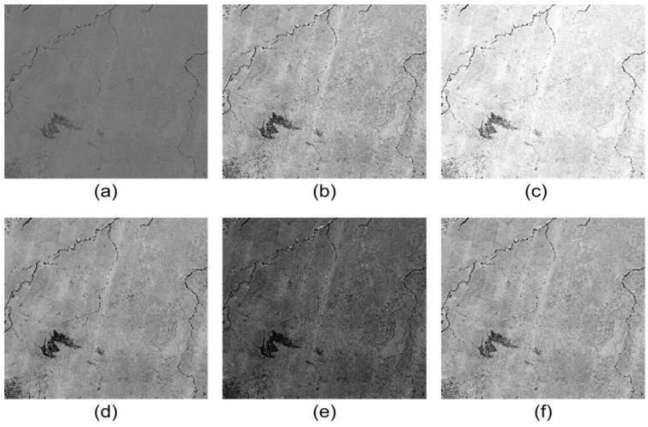

Figure 8: Sat: (a) Original (b) RHEDCT (c) HCTLS (d) GLIE (e) AEA (f) Proposed

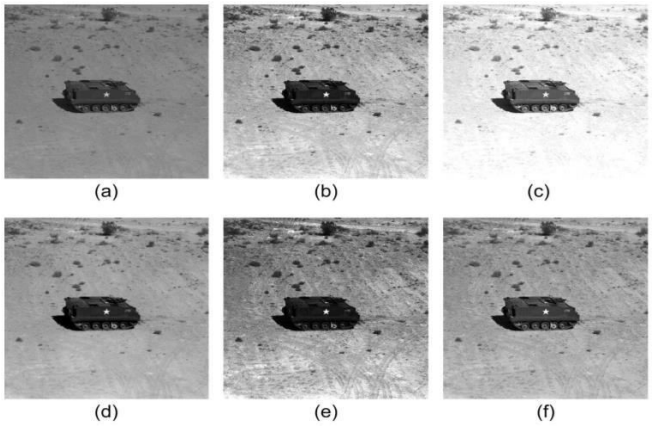

Figure 9: Tank: (a) Original (b) RHEDCT (c) HCTLS (d) GLIE (e) AEA (f) Proposed

6. Conclusion

This research introduces a new technique for remote sensing picture enhancement that can improve image visualization without over-enhancing the image. The image's details are extremely nicely highlighted by the Unsharp masking approach, and the clipping phenomena prevents the image from being too enhanced. The proposed method was tested on a number of photos, and the outcomes were compared to those of the other methods. The experimental findings demonstrate that our method provides the best image details and retains robustness across a variety of image formats. Specially if compared with the HCTLS method which is the last recent

proposed method, our method resolved the noise issue which was present in that method. When compared with the intensity graph our method clearly outperformed all the methods. If numerically compared than the values obtained for entropy, EME, MG and NIQE in our case are the best values as compared with the other methods. The proposed technique has its application in the classification of remote sensing images.

References:

1. Gonzalez R. C. and Woods R. E. (2008).,Digital Image Processing, 3rd ed, Prentice Hall,
2. Kim Y. T. (1997). Contrast enhancement using brightness preserving bi histogram equalization, IEEE Transactions on Consumer Electronics, 43(1), 1–8.
3. Lee E., Kim S., Kang W., Seo D. and Paik J. (2013). Contrast enhancement using dominant brightness level analysis and adaptive intensity transformation for remote sensing images, IEEE Geoscience and Remote Sensing Letters, 10(1), 62–66.
4. Celik T. (2014). Spatial entropy-based global and local image contrast enhancement, IEEE Transactions on Image Processing, 23(12), 5298–5308.
5. Celik T. and Tjahjadi T. (2011). Contextual and variational contrast enhancement, IEEE Transactions on Image Processing, 20(12), 3431–3441.
6. Atta R. and Ghanbari M. (2013). Low-contrast satellite images enhancement using discrete cosine transform pyramid and singular value decomposition, IET Image Processing, 7(5), 472-483.
7. Cao G., Zhao Y., Ni R. and Li X. (2014). Contrast enhancement-based forensics in digital images, IEEE Transactions on Information Forensics and Security,9(3), 515-525.
8. Demirel H., Ozcinar C. and Anbarjafari G.(2010). Satellite image contrast enhancement using discrete wavelet transform and singular value decomposition, IEEE Geoscience and Remote Sensing Letters, 7(2), 333-337.
9. Jang J. H., Kim S. D. and Ra J. B. (2011). Enhancement of optical remote sensing images by subband-decomposed multiscale retinex with hybrid intensity transfer function, IEEE Geoscience and Remote Sensing Letters, 8(5), 983-987.
10. Singh K and Kapoor R. (2014). Image enhancement using exposure based subimage histogram equalization, Pattern recognition letters, 36, 10-14.
11. Fu X., Wang J., Zeng D., Huang Y. and Ding X. (2015). Remote sensing image enhancement using regularized-histogram equalization and DCT, IEEE Geoscience and Remote Sensing Letters, 12(11), 2301-2305.
12. Liu J., Zhou C., Chen P. and Kang C. (2017). An efficient contrast enhancement method for remote sensing images, IEEE Geoscience and Remote SensingLetters, 14(10), 1715-1719.

13. Huang Z., Zhu Z., An Q., Wang Z. and Fang H.(2021). Global–local image enhancement with contrast improvement based on weighted least squares, Optik- International Journal for light and Electron Optics, 243(167433).
14. Wang R., Xiao W. (2022). Adaptive Enhancement Algorithm of High-Resolution Satellite Image Based on Feature Fusion, Journal of Mathematics, 2022(1029247).
15. Spring K., C. Russ John, Mathew J., Hill P., Fellers T. and Davidson M.W. (2016). Unsharp mask filtering, Interactive tutorials-Optical microscopy primer,
16. Ramponi G. (1998). A rational unsharp masking technique, Journal Electron Imaging, 7(2), 333-338.
17. Kotera H. and Wang H. (2005). Multiscale image sharpening adaptive to edge profile, Journal of Electronic Imaging, 14(1).
18. Kim Y. T. (1997). Contrast Enhancement Using Brightness Preserving Bi-Histogram Equalization, IEEE transactions on consumer electronics, 43(1),1-8.
19. Moon T. K. and Stirling W. C. (2000). Mathematical Methods and Algorithms for Signal Processing, Upper Saddle River, NJ: Prentice-Hall.
20. Agaian Sos S., Lentz K. P. and Grigoryam A. M. (2000). A new measure of image enhancement, IASTED International Conference on Signal Processing and Communication.
21. Mittal A., Soundararajan R. and Bovik A. C. (2013). Making a Completely Blind Image Quality Analyzer, IEEE signal processing letters, 20(3), 209-212.